Process Biochemistry 51 (2016) 542–553

Contents lists available at ScienceDirect

Process Biochemistry

journal homepage: www.elsevier.com/locate/procbio

Immunomodulatory effects of a polysaccharide purified from *Lepidium meyenii* Walp. on macrophages

Wei Wang[a], Ye Zou[a], Qian Li[a], Riwen Mao[b], Xingjun Shao[b], Dun Jin[c], Daheng Zheng[a], Ting Zhao[c], Huifen Zhu[b], Lin Zhang[b], Liuqing Yang[c,*], Xiangyang Wu[d,**]

[a] School of Food and Biological Engineering, Jiangsu University, Xuefu Rd. 301, Zhenjiang 212013, Jiangsu, China
[b] Nucell Biotechnology Co., Ltd., Jingsi Rd. 2, Zhenjiang 212009, Jiangsu, China
[c] School of Chemistry and Chemical Engineering, Jiangsu University, Xuefu Rd. 301, Zhenjiang 212013, China
[d] School of the Environment and Safety Engineering, Jiangsu University, Xuefu Rd. 301, Zhenjiang 212013, Jiangsu, China

ARTICLE INFO

Article history:
Received 13 October 2015
Received in revised form 12 January 2016
Accepted 18 January 2016
Available online 21 January 2016

Keywords:
Maca
Polysaccharides
Immunomodulatory
Macrophage activation

ABSTRACT

A polysaccharide (MP21) was extracted and purified from *Lepidium meyenii* Walp. using DEAE-52 and Sephacryl™ S-500 columns. Its physicochemical properties and macrophage immunomodulatory activity were investigated *in vitro*. The results indicated that MP21 had an average molecular weight of 3.68×10^5 Da and was mainly composed of rhamnose, arabinose and galactose in a molar ratio of 1:4.84:5.34. The conformation of MP21 was between a sphere and random coil, and different treatments could change its conformation and asymmetry. RAW264.7 murine macrophages treated with MP21 could significantly inhibit the proliferation of human hepatocellular carcinoma HepG-2. MP21 could enhance the phagocytic capacity and induce elevated NO, ROS, TNF-α, and IL-1β secretion in RAW264.7 in a dose-dependent manner. MP21 promoted the expression of both iNOS protein and mRNA. The expression of the NF-κB p65 protein was also up-regulated by MP21. These results suggest that MP21 could exert cytotoxicity towards HepG-2 by activating macrophages via the NF-κB signaling pathway.

1. Introduction

Immunomodulatory agents are substances that can stimulate immune responses or maintain immune balance [1]. Many reports have demonstrated that plant polysaccharides are ideal immunomodulators owing to their non-cytotoxic properties such as *Cordyceps taii* polysaccharide and *Hericium erinaceus* polysaccharide [2,3]. Macrophages play a crucial role in the immune system. They are the first cells to recognize infectious agents, and they are central to cell-mediated and humoral immunity. After activation, macrophages synthesize and secrete nitric oxide, reactive oxygen species and cytokines, which function as mediators of the immune system [4]. Immunomodulatory polysaccharides exhibit a variety of beneficial pharmacological effects via their ability to modulate macrophage immune function [5]. An increasing number of researchers have focused on the study and exploitation of botanical polysaccharides with macrophage immunomodulatory activity.

Lepidium meyenii Walp., known as 'maca', belongs to the family *Brassicae* and is cultivated mainly in the central Andes of Peru. It has been used as food and traditional medicine in the region for over 2000 years [6]. Recently, maca has received increasing research interest due to its pronounced widespread biological activities, such as improving sexual performance [7], antioxidant activity [8], preventing prostate hyperplasia [9], alleviating menopausal syndrome [10], antifatigue [11] and immunomodulatory effects [12]. However, recent studies of maca are mainly focused on the crude extract and some small molecular compounds, including glucosinolates [13], alkaloids [14] and sterols [15]. Investigations of high molecular weight constituents, *i.e.*, polysaccharides, have only focused on the extraction and antioxidant activity of crude polysaccharides [16]. Little attention has been devoted to the characterization and immunomodulatory activity of purified polysaccharides from maca. In this study, a polysaccharide of maca was isolated and purified. Its physicochemical properties and immunomodulatory effects on RAW264.7 were studied. Results of this study could instigate further research, and will ultimately help in developing novel functional foodstuff and drugs.

* Corresponding author. Fax: +86 511 88791800.
** Corresponding author. Fax: +86 511 88791200.
E-mail addresses: yangliuqing@ujs.edu.cn (L. Yang), wuxy@ujs.edu.cn (X. Wu).

http://dx.doi.org/10.1016/j.procbio.2016.01.003
1359-5113/

2. Materials and methods

2.1. Materials and reagents

The dry maca roots were purchased from Auka Biotechnology Co., Ltd. (Kunming, China) and identified by Chen Li (Chief Pharmacist, Food and Drug Administration Bureau of Zhenjiang). It was crushed and sieved on a 75 μm sieve.

DEAE-52 cellulose and Sephacryl™ S-500 were purchased from Whatman Co., Ltd. (Maidstone, UK). T-series dextrans were purchased from Amersham Pharmacia Biotechnology Co., Ltd. (Uppsala, Sweden). Rhamnose, arabinose, xylose, mannose, glucose, galactose, galacturonic acid, inositol, dimethylsulfoxide (DMSO), 3-(4,5-dimethylthiazol-2-yl)-2,5-diphenyl tetrazolium bromide (MTT), α-amylase, 5-fluorouracil (5-Fu) and Lipopolysaccharides (LPS) were purchased from Sigma Chemical Co. (Saint Louis, USA). Assay kits for interleukin-1β (IL-1β), tumor necrosis factor-α (TNF-α), nitric oxide (NO), reactive oxygen species (ROS) and BCA Protein were purchased from Nanjing Jiancheng Bioengineering Institute (Nanjing, China). RNA PCR kit (AMV) ver.3.0 and total RNAiso extraction reagent were purchased from Dalian TaKaRa Bio Group (Dalian, China). PVDF membrane was purchased from BIO RAD Co., Ltd. (Hercules, USA). Rabbit anti murine NF-κB p65, iNOS, β-actin antibody and HRP conjugated goat anti rabbit-IgG were purchased from Santa Cruz Biotechnology Co., Ltd. (Santa Cruz, USA). HepG-2 was purchased from Nanjing University (Nanjing, China). RAW264.7 was purchased from Institute of Cell Biology, Chinese Academy of Sciences (Shanghai, China). Cells were incubated in 5% CO_2 at 37 °C in DMEM medium supplemented with 10% fetal bovine serum, 100 IU/mL penicillin and 100 μg/mL streptomycin. All other reagents were of analytical grade.

2.2. Extraction and purification of maca polysaccharides

The maca powder was extracted three times with boiling water (1:20, (w/v)) for 4 h. After centrifugation (4000 × *g*, 20 min), the supernatant was collected and concentrated. Then the concentrated solution was treated with α-amylase to remove starch. After centrifugation (4000 × *g*, 20 min), the supernatant was mixed with four volumes of 95% ethanol and kept at 4 °C for 12 h. The precipitate was dissolved in deionized water and treated with trichloroacetic acid (TCA) to remove proteins. Finally, the deproteinized extract was dialyzed, concentrated and freeze-dried, affording the crude maca polysaccharide (MP). MP was re-dissolved in deionized water and loaded on a DEAE-52 cellulose column (1.6 × 50 cm), pre-equilibrated with deionized water and eluted with NaCl gradient solution (0–0.5 M) at a flow rate of 1 mL/min (6 mL/tube). Each elution fraction was collected and monitored according to the total carbohydrate content by the phenol-sulfuric acid method [17]. The major fraction, MP2, was further purified by Sephacryl™ S-500 column (1.6 × 50 cm), pre-equilibrated with deionized water and eluted with 0.1 M NaCl at a rate of 0.3 mL/min (6 mL/tube). The main fraction was collected, dialyzed and lyophilized to afford one white fluffy polysaccharide MP21.

2.3. General analysis

The total carbohydrate content was determined by the phenol-sulfuric acid method with D-glucose as standard [17]. The uronic acid content was measured according to mhydroxybiphenyl-sulphuric acid method with galacturonic acid as standard [18]. The protein content was evaluated by Bradford's method with bovine serum albumin (BSA) as standard [19].

2.4. Molecular weight determination

The molecular weight of MP21 was determined by high-performance gel-permeation chromatography (HPGPC) on a LC-10AVP HPLC system (Shimadzu, Tokyo, Japan) equipped with a refractive index detector (RID). TSK-GUARD PWH column (7.5 × 75 mm, Tosoh, Tokyo, Japan) was used as a pre-column, and TSK-GEL G4000PW column (7.5 × 300 mm, Tosoh, Tokyo, Japan) was used as a separation column. The column was eluted with 0.003 M CH_3COONa solution at a flow rate of 1 mL/min and calibrated with standard dextrans (T-10, T-40, T-70, T-500 and T-2000).

2.5. Neutral monosaccharide composition analysis

The neutral monosaccharide composition of MP21 was determined using the method reported by Yang et al [20] with slight modification. Briefly, MP21 (5 mg) was hydrolyzed with 3 M H_2SO_4 (3 mL) at 110 °C for 8 h. Then the hydrolysate was neutralized with $BaCO_3$ and the supernatant was collected and lyophilized. The lyophilized product was reacted with thydroxylamine hydrochloride (5 mg), cyclohexanhexol (5 mg), pyridine (0.5 mL) and acetic anhydride (0.5 mL) at 90 °C for 1 h. The monosaccharide standards including rhamnose, arabinose, xylose, mannose, glucose and galactose were acetylated in the same way. Finally, the acetylated samples were analyzed with GC-2010 system (Shimadzu, Tokyo, Japan), equipped with an HP-5MS column (0.25 mm × 30 m × 0.25 μm, Tosoh, Tokyo, Japan) and a flame-ionization detector. The temperature was set as follows: the initial temperature of the column was 130 °C, maintained for 5 min and then increased to 240 °C at 4 °C/min. The 240 °C was maintained for 5 min. The flow rate of N_2, H_2 and air were 50, 37 and 370 mL/min, respectively.

2.6. UV and FT-IR spectroscopy analysis

The UV spectrum of MP21 was recorded with a UV-2450 spectrophotometer (Shimadzu, Tokyo, Japan) in the wavelength range of 190–400 nm. The FT-IR spectrum was recorded with a Nicolet Nexus 470 FT-IR spectrophotometer (Thermo Nicolet, Madison, USA) in the wavenumber range of 4000–400 cm^{-1}.

2.7. Circular dichroism (CD) spectroscopy analysis

MP21 was dissolved in deionized water at a concentration of 1 mg/mL. CD was performed on a JASCO J-815 spectropolarimeter (JASCO, Tokyo, Japan). Spectra were recorded with the following setup: wavelength of 190–250 nm, bandwidth of 2.5 nm, time constant of 2 s and scan rate of 50 nm/min.

2.8. Atomic force microscopy (AFM) analysis

MP21 was dissolved in deionized water at a concentration of 1 mg/mL. The solution (5 μL) was dropped onto a freshly cleaved mica surface and allowed to dry at room temperature. AFM was performed in the tapping-mode using a MFP-3D instrument (Asylum Research, Santa Barbara, USA).

2.9. Size exclusion chromatography coupled with multi-angle laser light scattering (SEC-MALLS) analysis

The SEC-MALLS system consisted of three separation columns (SB-803, SB-804 and SB-805, Shodex, Tokyo, Japan), a separation module (Waters 1100, Milford, USA) and a multi-angle laser light scattering detector (Wyatt DAWN HELEOS-II, Santa Barbara, USA) with a laser at 633 nm, along with a refractive index monitor (Agilent 1100, Santa Clara, USA). MP21 was dissolved in 0.1 M NaCl

solution at a concentration of 1 mg/mL, and the solution filtered with a 0.22 μm microporous membrane. 100 μL of MP21 solution was injected into the system and eluted with 0.1 M NaCl at 0.4 mL/min. Data for molecular weight, distribution and chain conformation were analyzed by ASTRA software (Version 4.73.04, Wyatt, Santa Barbara, USA) using a dn/dc of 0.125 mL/g.

2.10. Cells proliferation assay

HepG-2 (4×10^4 cells/mL, 100 μL/well) was seed in 96-well plate and incubated for 24 h. Then the supernatant was discarded, DMEM, MP21 (62.5–1000 μg/mL) or 5-Fu (50 μg/mL) were added [21]. After 48 h of incubation, the supernatant was removed and 100 μL of combined MTT (dissolved MTT into D-Hanks solution, 1 mg/mL) was added into each well and incubated for 4 h. The supernatant was then removed and 100 μL of DMSO was added. After 1 h incubation period, the absorbance at 570 nm was detected by a microplate ELISA reader (Spectra MAX 190, Sunnyvale, Molecular Devices, USA).

2.11. Macrophage-mediated cytotoxicity assay

RAW264.7 (2×10^5 cells/mL, 100 μL/well) was seeded in 96-well plate and incubated for 24 h. Then the supernatant was discarded, DMEM, MP21 (62.5–1000 μg/mL) or LPS (10 μg/mL) were added and incubated for 48 h. The culture medium was collected and centrifuged (1500 *g*, 15 min). The supernatant (P-MΦ-CM) was then collected after centrifugation. HepG-2 (2×10^4 cells/mL, 100 μL/well) was seeded into 96-well plate and incubated for 24 h. P-MΦ-CM was added to the HepG-2 and incubated for another 48 h. The MTT method described in 2.10 was used to detect the cell viability. Simultaneously, the adherent cell of RAW264.7 (MΦ), which contributed as effecter cells were washed twice with a preheating culture solution and co-incubated with 100 μL HepG-2 (2×10^4 cells/mL) for 48 h to investigate the cytotoxicity of RAW264.7.

2.12. Phagocytic capacity assay

The phagocytic activity of macrophage was measured by the neutral red uptake method. Briefly, cells were incubated with DMEM, MP21 (62.5–1000 μg/mL) or LPS (10 μg/mL) for 48 h, then the supernatants were removed, 100 μL of neutral red solution (dissolved in 10 mM PBS, 0.075%) was added and incubated for further 4 h. The plate was washed three times with PBS. 100 μL of the cell lysis buffer (ethanol: glacial acetic acid = 1:1, (v/v)) was added and incubated at 4 °C for 2 h, with absorbance detected at 540 nm by a microplate ELISA reader (Spectra MAX 190, Molecular Devices, Sunnyvale, USA).

2.13. NO, TNF-α and IL-1β secretion assay

RAW264.7 (2×10^5 cells/mL, 500 μL/well) was added in 24-well plate and stimulated with DMEM, MP21 (62.5–1000 μg/mL) or LPS (10 μg/mL) for 48 h. The isolated supernatants were collected for NO, TNF-α and IL-1β quantification. The NO contents in the supernatants were estimated by measuring nitrite levels with NO test kits (Nanjing Jiancheng, Nanjing, China). The absorbance was read at 540 nm by a microplate ELISA reader (Spectra MAX 190, Molecular Devices, Sunnyvale, USA). The concentrations of nitrite were determined from a least squares linear regression analysis of a sodium nitrite standard curve. The cytokine (IL-1β and TNF-α) levels in the supernatants were determined by commercial ELISA kits according to the manufacturer's instructions. The absorbance was measured at 450 nm by a microplate ELISA reader (Spectra MAX 190, Molecular Devices, Sunnyvale, USA). The concentrations of IL-1β and TNF-α were calculated according to the standard curve using each of the recombinant cytokines in the ELISA kits (Nanjing Jiancheng, Nanjing, China).

2.14. ROS secretion assay

ROS production by RAW264.7 was measured using 2, 7-dichlorofuorescin diacetate (DCFH-DA). RAW264.7 (1×10^5 cells/well, 100 μL/well) was seeded in 96-well plate and incubated overnight. Cells were treated with DMEM, MP21 (62.5–1000 μg/mL) or LPS (10 μg/mL). After 24 h, all culture medium was carefully removed, followed by the addition of 100 μL of 10 μM DCFH-DA in serum free medium. After a 30 min incubation at 37 °C, the dye was removed, and the cells were washed twice with PBS. Fluorescence intensity was measured using a microplate reader (BioTek, Winooski, USA) at 485 nm for excitation and 520 nm for emission.

2.15. Western blot assay

The iNOS protein expression of RAW264.7 was performed on whole-cell extracts. RAW264.7 (2×10^5 cells/mL, 2 mL/well) was seeded into 6-well plate and treated with DMEM, MP21 (62.5–1000 μg/mL) or LPS (10 μg/mL) for 48 h. The medium was removed and the adherent cells washed twice with 1 mL ice-cold PBS. Then 500 μL of pancreatin was added to digest adherent cells. The supernatant was discarded and the cells resolved in 1 mL ice-cold Hanks, then centrifuged (1500 *g*, 5 min) at 4 °C. 100 μL of lysis buffer (10 mM HEPES, 150 mM NaCl, 1 mM EGTA, 1% CHAPS and 1% Triton X-100) containing 1% of protease inhibitor cocktail was added to the precipitate, and then left on ice for 30 min. The solution was centrifuged (12,000 *g*, 6 min) at 4 °C. The protein concentration of supernatant was determined by BCA Protein Assay kit and stored at −80 °C. The extracted protein was boiled with isotonic loading buffer for 5 min followed by the separation of protein (20 μg) by 12% SDS-polyacrylamide gelelectrophoresis (SDS-PAGE) which was transferred onto PVDF membrane. The membrane was blocked with 5% skim milk with TBST for 1 h at room temperature and incubated with rabbit anti murine iNOS and β-actin antibody overnight at 4 °C. After washing twice with TBST (15 min/time), the membrane was incubated with HRP conjugated goat anti rabbit-IgG for 2 h, and the antibody-specific protein was visualized by enhanced chemiluminesence detection system with ECL kit.

NF-κB p65 protein using nuclear extracts was also performed as above with β-actin as internal reference. The lysis buffer contains 20 mM Tris (pH 7.5), 2 mM EDTA, 135 mM NaCl, 2 mM DTT, 2 mM sodium pyrophosphate, 25 mM β-glycerophosphate, 10% glycerol, 1% Triton X-100, 1 mM Na_3VO_4, 10 mM NaF, 10 μg/mL leupeptin, 10 μg/mL aprotinin and 1 mM PMSF. The primary antibody was rabbit anti murine NF-κB p65 and β-actin antibody, and the secondary antibody was HRP conjugated goat anti rabbit-IgG.

2.16. RT-PCR

RAW264.7 (2×10^5 cells/mL, 1 mL/well) was seeded into 6-well plate, then treated with DMEM, MP21 (250–1000 μg/mL) or LPS (10 μg/mL) and incubated for 48 h. Total RNA was extracted using Trizol total RNA extraction kit according to the manufacturer's protocol. Expression levels of iNOS and β-actin were determined by RT-PCR using the RNA PCR kit (AMV) Ver.3.0. The cDNA was amplified by Polymerase Chain Reaction (PCR) using Ex Taq HS and cytokines primer. The sequence of the cytokines primes was as below: FP5-CCCTTCCGAAGTTTCTGGCAGCAGC-3, RP5-GGCTGTCAGAGCCTCGTGGCTTTGG-3 for iNOS; FP5-TGGAATCCTGTGGCATCCATGAAAC-3, RP5-TAAAACGCAGCTCAGTAACAGTCCG-3 for β-actin. PCR reactions

were performed as follows: initial denaturation at 94 °C for 3 min, 25 cycles of denaturation (94 °C for 30 s), annealing (56 °C for 40 s) and extension (72 °C for 10 min) and the final extension step at 4 °C for 10 min. Amplification products were separated in 2% (w/v) agarose gels stained with loading buffer and visualized with UV light.

2.17. Statistical analysis

Data from the analysis were presented as mean ± S.D. Statistical analyses were carried out by SPSS version 16.0 (SPSS, USA). One-way analysis of variance (ANOVA) for statistical analysis and the Tukey method for multiple comparisons among the groups were used. Significant differences were set at $P < 0.05$ and $P < 0.01$.

3. Results and discussion

3.1. Isolation, purification and chemical composition of MP21

P21 sed rides 00 columns. The MP yield was 5.71% based on the dried maca powder used. MP was then purified with a DEAE-52 column, the elution profile indicated that MP was mainly composed of MP1, MP2, MP3, MP4 and MP5 (Supplementary Fig. S1A), and the yields were 22.1%, 35.7%, 20.3%, 8.2% and 3.7%, respectively. MP2 was the major fraction. A further separation of MP2 was performed on a Sephacryl™ S-500 column. As shown in Supplementary Fig. S1B, one main fraction, named MP21, with a yield of 59.3% was collected for further characterization of the physicochemical properties and bioactivity. The total carbohydrate and uronic acid contents of MP21 were 90.5% and 39.1%, respectively. MP21 showed negative responses to the Bradford test. The HPGPC profile of MP21 is shown in Supplementary Fig. S2, a single and symmetrical peak indicated a high purity for the MP21 sample, and the average molecular weight of MP21 was calculated as 3.68×10^5 Da. The neutral monosaccharide composition of MP21 is shown in Fig. 1A, 1B. Rhamnose, arabinose and galactose were the major groups in a molar ratio of 1:4.84:5.34, respectively.

3.2. FT-IR spectroscopy analysis of MP21

The FT-IR spectrum of MP21 is presented in Supplementary Fig. S3. The spectrum exhibited the typical signals of polysaccharide in the range of 4000–400 cm^{-1}. A broad and strong peak at approximately 3423 cm^{-1} was attributed to the O—H stretching vibration and the presence of intermolecular hydrogen bonds in polysaccharide [22,23]. The peaks appearing at 1618 cm^{-1} and 1047 cm^{-1} could be contributed to the C=O asymmetric stretching [24]. The peak at 2932 cm^{-1} corresponded to C—H stretching vibration, the characteristic peak of polysaccharides [23]. The region of 1000–1200 cm^{-1} was attributed to the C—OH side groups and C—O—C glycosidic band stretching vibrations [25]. The peak at 1420 cm^{-1} corresponded to CH deformation vibration, and the 775 cm^{-1} peak was characteristic of pyranose [22].

3.3. CD spectroscopy analysis of MP21

The CD studies have been extensively applied to determine the structural characteristics of carbohydrates [26]. Supplementary Fig. S4 shows the CD spectra of MP21 with different treatments, which induced changes in the MP21 conformation. Supplementary Fig. S4A displays the conformation variation of MP21 after the thermal treatments at 60 °C and 100 °C. The intensity of the positive peak at 195 nm was enhanced, and the peak position was not changed, indicating that the type of asymmetric structure repeating unit was unchanged. As shown in Supplementary Fig. S4B, when the pH value was adjusted to 12, strengthening and a positive Cotton effect occurred in the positive peak at 192 nm. A stronger negative Cotton effect was found when the pH value was 2. These findings might be due to elimination reactions of polysaccharides in acidic or alkaline conditions [27]. The results demonstrated that strong acid and alkali conditions could cause a conformation transformation in MP21, but acid treatment had a more significant influence on MP21 than alkali treatment. To investigate the polysaccharide conformation changes influenced by ionic strength, Ca^{2+} was added into polysaccharide solution. The peak intensity of MP21 became stronger at 208 nm. This suggested that Ca^{2+} interacted with some carboxyl groups in polysaccharide chains, leading to a partial chain polymerization in MP21. Thus, the structure of MP21 was altered and had an increasing appearance of asymmetry in the presence of Ca^{2+} (Supplementary Fig. S4C) [28]. The effect of urea on MP21 conformation is shown in Supplementary Fig. S4D. There was a positive Cotton effect at 197 nm, indicating that urea greatly influenced the structure of MP21 and increased asymmetry. After treatment with Congo red, polysaccharide MP21 showed no obvious positive Cotton effect from 230 to 240 nm. This result indicated that MP21 was disordered and could not form a complex with Congo red. There was also no obvious negative Cotton effect for the peaks at 206 and 208 nm, which further suggested that MP21 had a random coil-chain conformation in aqueous solution (Supplementary Fig. S4E) [29].

3.4. AFM analysis of MP21

The MP21 morphology was observed by AFM to obtain the direct chain conformation of the polysaccharides. As shown in Fig. 1C, polysaccharide chains formed tangled agglomerates that vary in size. The height of a single polysaccharide chain was approximately 0.1–1 nm, and the height of MP21 was approximately 2–15 nm (Fig. 1D,E) [30]. This result indicated that the structure of MP21 was branched, with polysaccharide chains entangled with each other.

3.5. SEC-MALLS analysis of MP21

Fig. 1F shows light scattering and refractive index (RI) chromatograms of MP21. The RI signal of the polysaccharide exhibited a single and symmetrical peak, indicating it was a homogeneous component. The M_w, M_n and M_z values of MP21 were 7.074×10^4, 4.212×10^4 and 2.255×10^4 g/mol, and the R_w, R_n and R_z were 51.8, 29.4 and 126.6 nm, respectively. The M_w/M_n value of MP21 was 1.680. These data indicated that the polysaccharide had a narrow molar mass distribution [31]. The chain conformation of MP21 in 0.1 M NaCl aqueous solution can be characterized based on the theory of dilute polymer solutions. The power law function $\langle S^2 \rangle_z^{1/2} = kM_w^{\nu}$ can be estimated from many experimental points in the SEC-MALLS chromatogram, which can reflect the chain conformation of polysaccharides in aqueous solution. Generally, the ν exponents of 0.33, 0.50–0.60 and 1.0 reflect the polymer molecular shape as sphere, random coil and rigid rod, respectively [32]. The ν of MP21 was 0.40, as calculated by ASTRA software, which indicated that the chain conformation of MP21 was between a sphere and random coil in the 0.1 M NaCl aqueous solution.

3.6. Effect of MP21 on HepG-2 cells

The cytotoxicity of MP21 towards HepG-2 cells *in vitro* was examined. However, MP21 was not able to inhibit the proliferation of HepG-2 cells at the tested concentrations (62.5–1000 μg/mL) (data not shown). Thus MP21 had no obvious toxic effect on HepG-2 cells. It has been reported that the polysaccharides from *Enteromorpha prolifera* exhibited growth inhibition on cancer cell lines such as AGS and DLD-1 cells. However, they were strong immunomod-

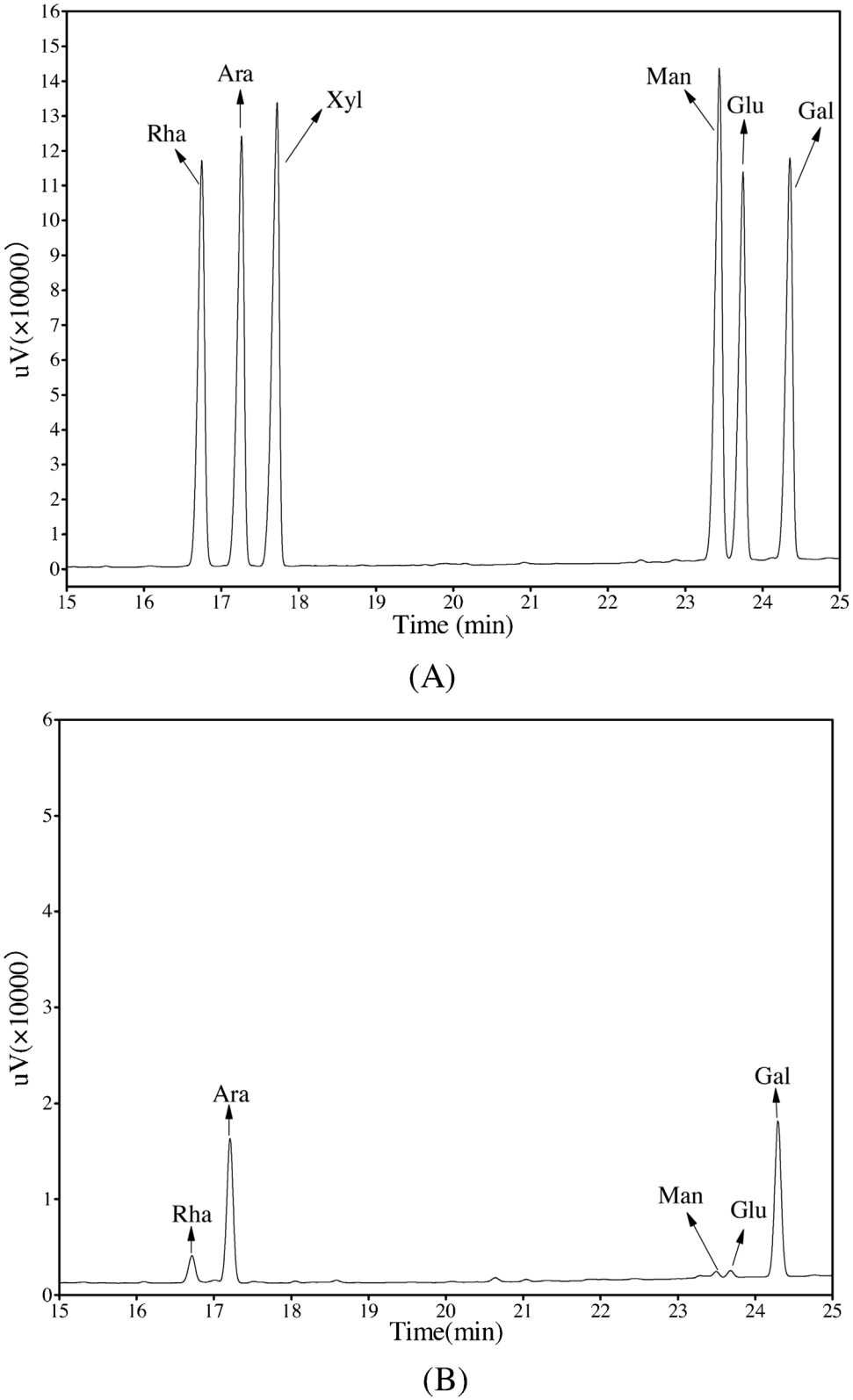

Fig. 1. (A) GC chromatogram of standard monosaccharides; (B) GC chromatogram of MP21; (C) AFM 2D map of MP21; (D) AFM 3D map of MP21; (E) AFM section analysis of MP21; (F) SEC-MALLS spectrum of MP21.

ulators, implying their potential anticancer activity *in vivo* through boosting the immune system [33]. Wang et al. also reported that the anti-tumor effect of a ganoderic acid from the medicinal mushroom Ling-zhi was related to its immunomodulating effect [34].

RAW264.7 is a kind of murine macrophage cell. The MTT assay was used to evaluate the toxic effect of MP21 on RAW264.7. MP21 has no toxicity on RAW264.7 (data not shown). Thus, it had been selected as test cells in the following study.

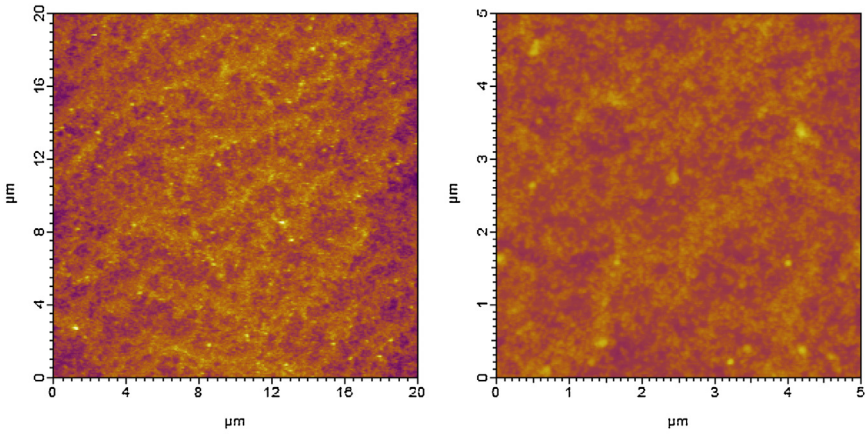

(C)

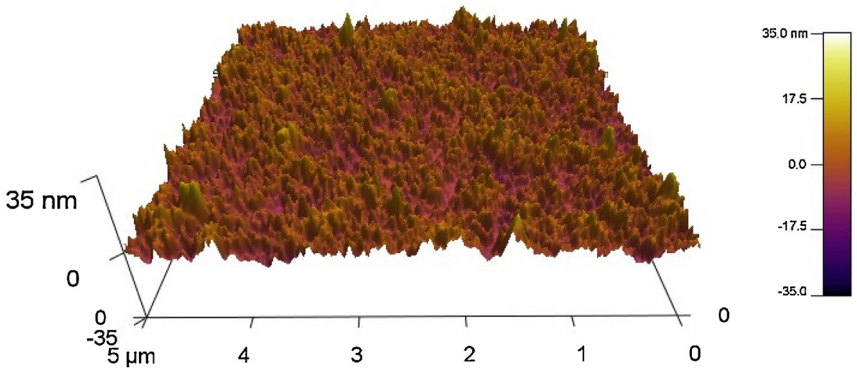

(D)

Fig. 1. (*Continued*)

3.7. Effect of macrophage-mediated cytotoxicity towards HepG-2 cells

As seen in Fig. 2A, macrophages induced by MP21 significantly inhibited the proliferation of HepG-2 tumor cells compared with normal control macrophages ($p < 0.01$), the maximum effect induced by MP21 at a concentration of 1000 μg/mL was nearly 2-fold the effect of normal control macrophages. The cytotoxicity effect of cultured supernatant (P-MΦ-CM) is shown in Fig. 2A. MP21-treated P-MΦ-CM significantly inhibited the proliferation of HepG-2 in a distinct dose-dependent manner ($p < 0.05$, $p < 0.01$). Moreover, the effect of MP21 at 1000 μg/mL was nearly identical with the effect of LPS. The cytotoxicity of ΦM and P-MΦ-CM stimulated by MP21 was higher than that stimulated by *Grifola frondosa* polysaccharide reported by Mao et al. who had evaluated the macrophage cytotoxicity in the same experimental conditions [35]. Thus, MP21 exhibited an indirect cytotoxicity towards HepG-2 cells by stimulating macrophage responses, and the macrophage immunomodulatory activity is an important mechanism of MP21 antitumor activity.

3.8. Effect of MP21 on phagocytosis in RAW264.7 cells

One of the most distinguished features of activated macrophages is an increase in phagocytosis [36]. which represents the first and indispensable step in the response of macrophages to pathogens and cancer cells [1]. The effect of MP21 on phagocytosis by RAW264.7 is depicted in Fig. 2B. The results showed that MP21 significantly increased the phagocytosis of RAW264.7 in a dose-dependent manner. The phagocytic OD values of RAW264.7 under MP21 treatments exceed 1.75 from 250 μg/mL, it is better than the polysaccharide from *Schisandra chinensis* (Turcz.) Baill, which was 1.75 at 1000 μg/mL [37]. Moreover, the resulting OD value from treatment with 1000 μg/mL MP21 was greater than that with LPS treatment. Phagocytes act as regulatory and effector cells in the immune system. The enhancement of the phagocyte function by MP21 hence leads to the increasing innate immune response in resisting foreign materials, such as pathogens and tumor cells [38]. These results suggested that MP21 could prime macrophages for enhanced phagocytic capacities.

3.9. Effects of MP21 on NO secretion and iNOS expression in RAW264.7 cells

NO has been identified as a major effector molecule produced by macrophages and is involved in the regulation of apoptosis and in host defenses against microorganisms and tumor cells [38]. The synthesis of NO by activated macrophages is an important cytotoxic/cytostatic mechanism of non-specific immunity [39]. As shown in Table 1, after incubating the RAW264.6 with MP21 for 48 h, NO production was significantly stimulated in a dose-dependent manner, and the production of NO was significantly increased 3.68-fold than that in the control by MP21 at 1000 μg/mL ($p < 0.01$), Lee et al. found that RAW264.7 treated with polysaccharide from *Cordyceps militaris* culture broth showed 1.6-fold increase than that in the control at 1000 μg/mL [40]. Moreover, the effect

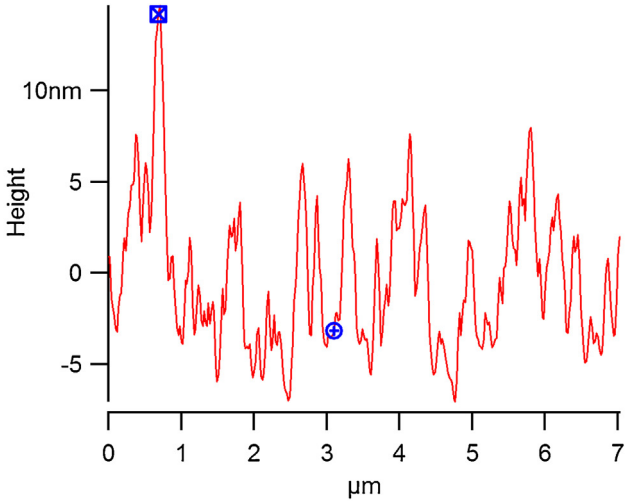

(E)

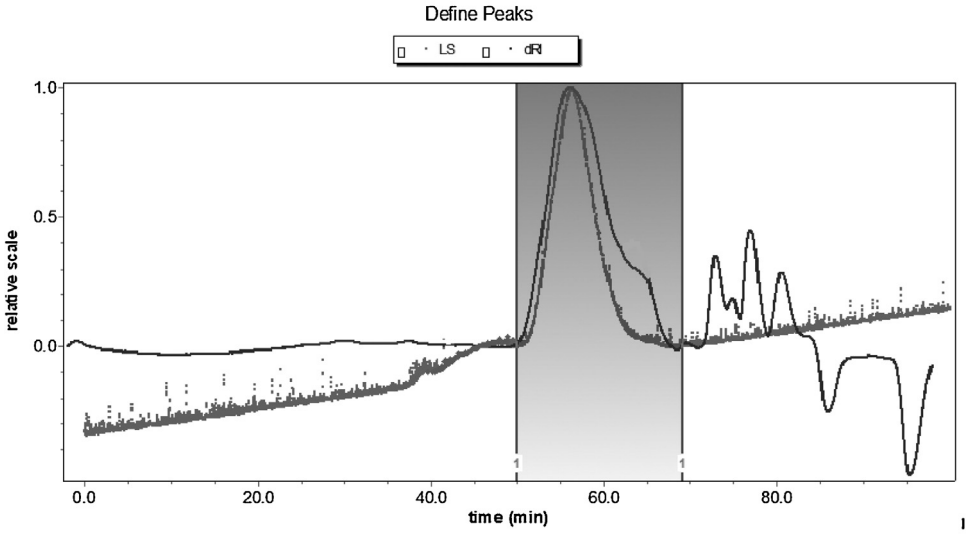

(F)

Fig. 1. (*Continued*).

Table 1
Effect of MP21 on NO, TNF-α and IL-1β secretion of RAW264.7. RAW 264.7 (2×10^5 cells/mL) was stimulated with DMEM as a normal control, LPS (10 μg/mL) or different concentrations of MP21 (62.5–1000 μg/mL) for 48 h.

Groups	NO level (μmol/L)	TNF-α level (pg/mL)	IL-1β level (pg/mL)
Normal control	2.63 ± 0.38	194.23 ± 11.25	105.55 ± 2.61
MP21 (62.5 μg/mL)	2.73 ± 0.47	214.28 ± 16.90	115.82 ± 6.84
MP21 (125 μg/mL)	3.07 ± 0.75	229.74 ± 8.47	135.90 ± 3.42
MP21 (250 μg/mL)	3.74 ± 0.72	309.19 ± 14.28^{aa}	205.03 ± 16.35^{aa}
MP21 (500 μg/mL)	4.35 ± 0.88	368.84 ± 22.01^{aa}	206.74 ± 18.54^{aa}
MP21 (1000 μg/mL)	9.69 ± 1.54^{aa}	430.64 ± 16.51^{aa}	218.09 ± 29.21^{aa}
LPS	11.14 ± 1.19^{aa}	340.80 ± 12.31^{aa}	206.43 ± 27.71^{aa}

The supernatant NO, TNF-α and IL-1β levels were determined using commercial test kit. Each value is presented as mean ± S.D. ($n = 5$). $^{aa}P < 0.01$ compared to normal control group.

at 1000 μg/mL of MP21 was nearly identical with that of LPS. The increasing production of NO suggested that MP21 may activate the bactericidal and tumoricidal activity of macrophages.

In living organisms, the NO synthase (NOS) consists of neuronal NOS (nNOS), endothelial NOS (eNOS) and induced NOS (iNOS). Among the three isoforms, iNOS is the most important key enzyme in NO synthesis. The production of NO via iNOS is crucial for killing tumor cells, infected cells and some pathogens in macrophages [41]. Based on the ability of MP21 to induce NO release, we evaluated whether this response was associated with the iNOS expression by determining the expression of iNOS protein and mRNA in the MP21-treated macrophages. As shown in Fig. 3A, MP21 increased iNOS protein levels in a concentration-dependent manner. MP21 significantly increased iNOS protein levels from 500 μg/mL ($p < 0.01$) and was almost equivalent to that in LPS at 1000 μg/mL (Fig. 3B). Simultaneously, the transcription level of

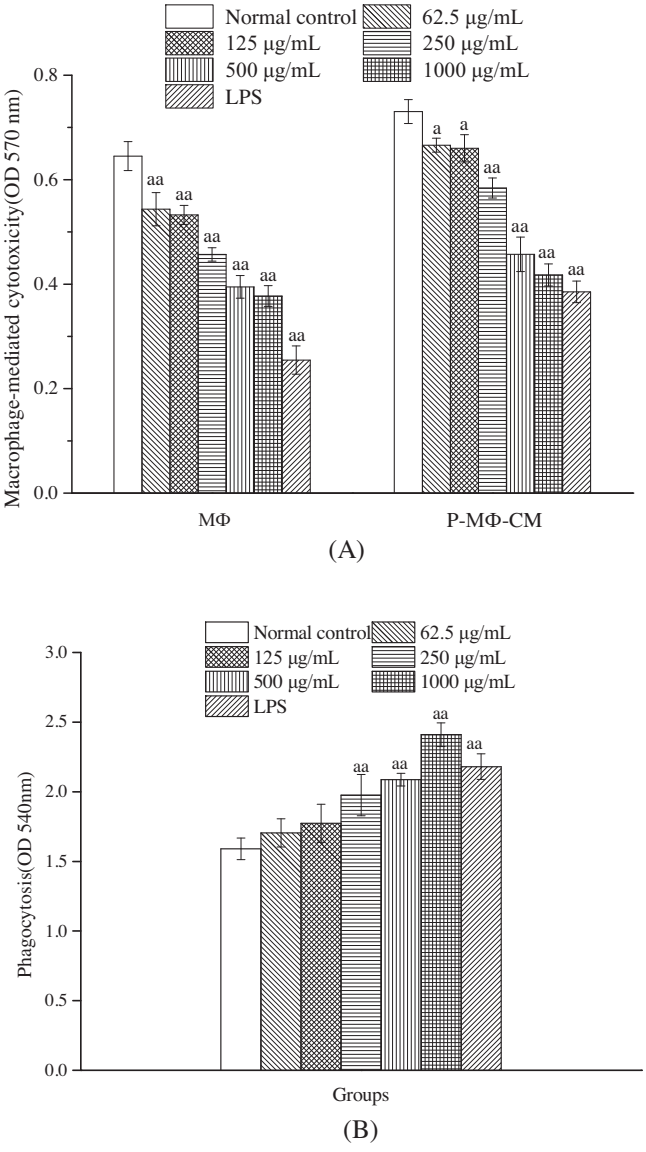

Fig. 2. (A) Macrophage-mediated cytotoxicity of activated RAW264.7 (MΦ) and cultured supernatant (P-MΦ-CM) towards HepG-2 tumor cells; (B) Effect of MP21 on phagocytosis activity of RAW264.7. Each value is presented as mean ± S.D. ($n = 5$). $^{a}P < 0.05$ compared to normal control group. $^{aa}P < 0.01$ compared to normal control group.

iNOS mRNA was also altered in a dose-dependent manner (Fig. 3C), and MP21 significantly increased iNOS mRNA levels at doses of 500 μg/mL and up ($p < 0.05$) (Fig. 3D). These results were consistent with iNOS protein expression and NO production. Given the above findings, these results suggest that MP21 most likely increases NO production via the upregulation of iNOS expression at the protein and gene levels.

3.10. Effects of MP21 on TNF-α and IL-1β secretion in RAW264.7 cells

Cytokines are intercellular signaling proteins released by both immune and non-immune cells. They play important roles in controlling the homeostasis of the whole organism by the induction of cell differentiation, proliferation and apoptosis, as well as defense functions, such as immune responses and inflammatory reactions. Cytokines are important in immune responses and play a pivotal role in fighting against tumor growth. The induction of cytokine synthesis is one method to evaluate the augmentation activity of innate immunity. Activated macrophages could generate and sequentially secrete a variety of proinflammatory cytokines, such as TNF-α and IL-β [42]. To evaluate the effects of MP21 on cytokine secretion in RAW264.7 macrophages, ELISA assays were performed to measure TNF-α and IL-β levels in culture supernatants of RAW264.7 treated with MP21. As shown in Table 1, MP21 increased the secretion of TNF-α and IL-β in a dose-dependent manner, the secretion levels of TNF-α and IL-β were significantly increased after treatment with 250, 500 and 1000 μg/mL MP21 ($p < 0.01$). Moreover, the secretion levels of TNF-α at 500 and 1000 μg/mL and IL-β at 1000 μg/mL were higher than with LPS treatment. At 125 μg/mL, the release of TNF-α was enhanced by 18.3% and at 250 μg/mL IL-β was enhanced by 94.2% compared to the control group. Fang et al. reported that the polysaccharide from *Laminaria japonica* at the concentration of 200 μg/mL can caused a 13.8% and 75.0% increase in the production of TNF-α and IL-1β [43]. The effect of MP21 on cytokine production further indicated that MP21 effectively activated macrophages.

3.11. Effects of MP21 on ROS production in RAW264.7 cells

ROS synthesized by NADPH oxidase acts as secondary messengers in many cellular processes, including signal transduction, redox signaling, autophagy and respiratory burst. In macrophages, ROS is a key functional effector of differentiation, activation and function. A consequence of heightened ROS synthesis is the activation of the MAPK and NF-κB signaling pathways, the activation of these pathways increases the expression of proinflammatory mediators [44]. The generation of ROS by MP21 was assessed by measuring DCF fluorescence. The fluorescence intensity in cells treated with MP21 was significantly increased in a dose-dependent manner (Fig. 4A), which was confirmed under fluorescence microscopy (Fig. 4B). When compared with the control group, the fluorescence intensity was noticeably enhanced ($p < 0.01$), and the highest activity was exhibited at 1000 μg/ml, which presented a 2.8-fold enhancement compared to the control (Fig. 4A). This result demonstrated that MP21 treatment mediated the upregulation of intracellular ROS production. Lee et al. determined the fluorescence intensity of *Cordyceps militaris* polysaccharide CM (500 μg/mL), which represented a 1.4-fold enhancement compared with that of the control treatment in RAW264.7 [42], while the fluorescence intensity of this study was higher than that reported by Lee et al. at same concentration. It may also be partly explained by the increased NO level caused by MP21 treatment. The surplus NO competed with oxygen, causing the displacement of oxygen from cytochrome-c oxidase, which led to a limitation in the rate of transfer in the electron transport chain, thus resulting in the generation of ROS [45].

Macrophages activation plays critical roles in host defense, including phagocytosis of pathogens and apoptotic cells, production of cytokines, proteolytic processing and presentation of foreign antigens. A variety of plant polysaccharides have been reported to exhibit beneficial pharmacological effects via their ability to modulate macrophage function. In particular, these compounds have been shown to increase macrophage cytotoxic activity against tumor cells, activate phagocytic activity, increase ROS and NO production and enhance secretion of cytokines and chemokines, such as TNF-α and IL-1β [46]. MP21 had no direct cytotoxicity towards tumor cells, but the cultural supernatant of macrophages treated with MP21 could kill HepG-2 cells. MP21 could also promote the releases of TNF-a, IL-1β, NO and ROS by macrophages, indicating that MP21 polysaccharides may indirectly play the role of antitumors through the releases of effector molecules by macrophages. Therefore, MP21-mediated activation of macrophages and production of various effector molecules may contribute to its antitumor

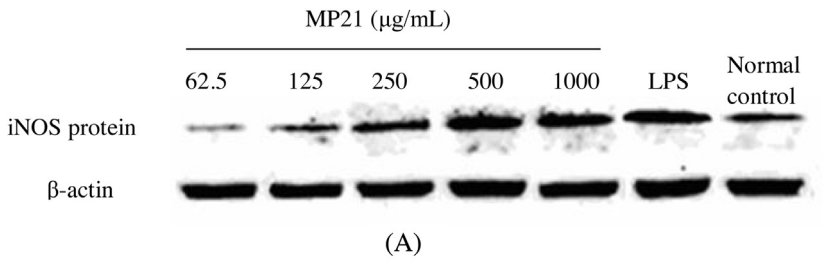

(A)

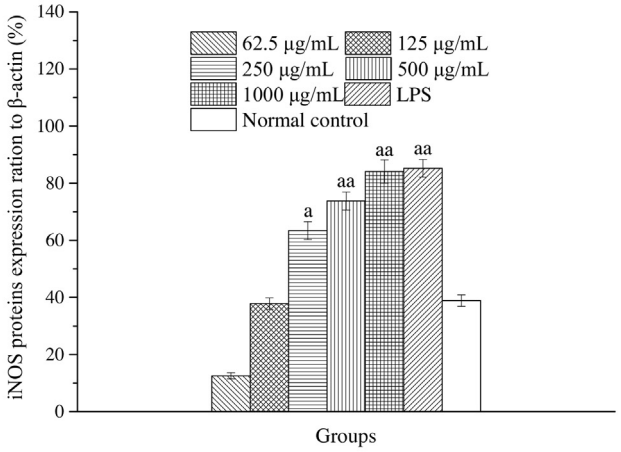

(B)

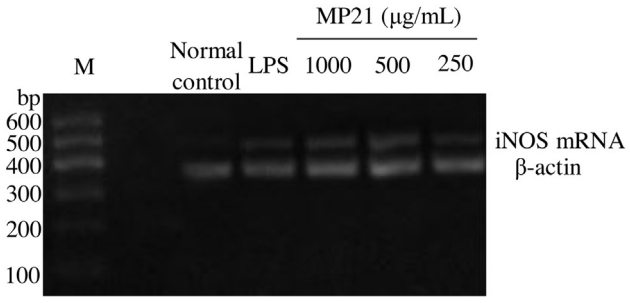

(C)

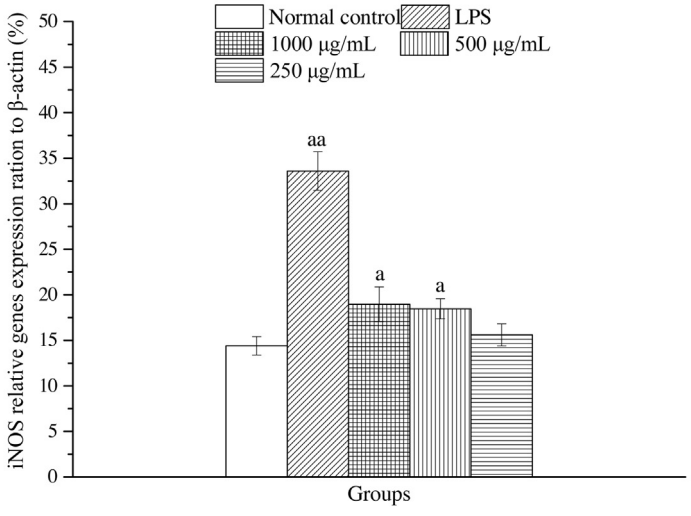

(D)

Fig. 3. (A) Effect of MP21 on the iNOS protein expression level in RAW264.7; (B) Densitometry analyses are presented as iNOS proteins expression ratio to β-actin using Quantity One software; (C) Effect of MP21 on the iNOS mRNA expression level in RAW264.7; (D) Densitometry analyses are presented as iNOS genes expression ratio to β-actin using Quantity One software. $^{a}P < 0.05$ compared to normal control group. $^{aa}P < 0.01$ compared to normal control group.

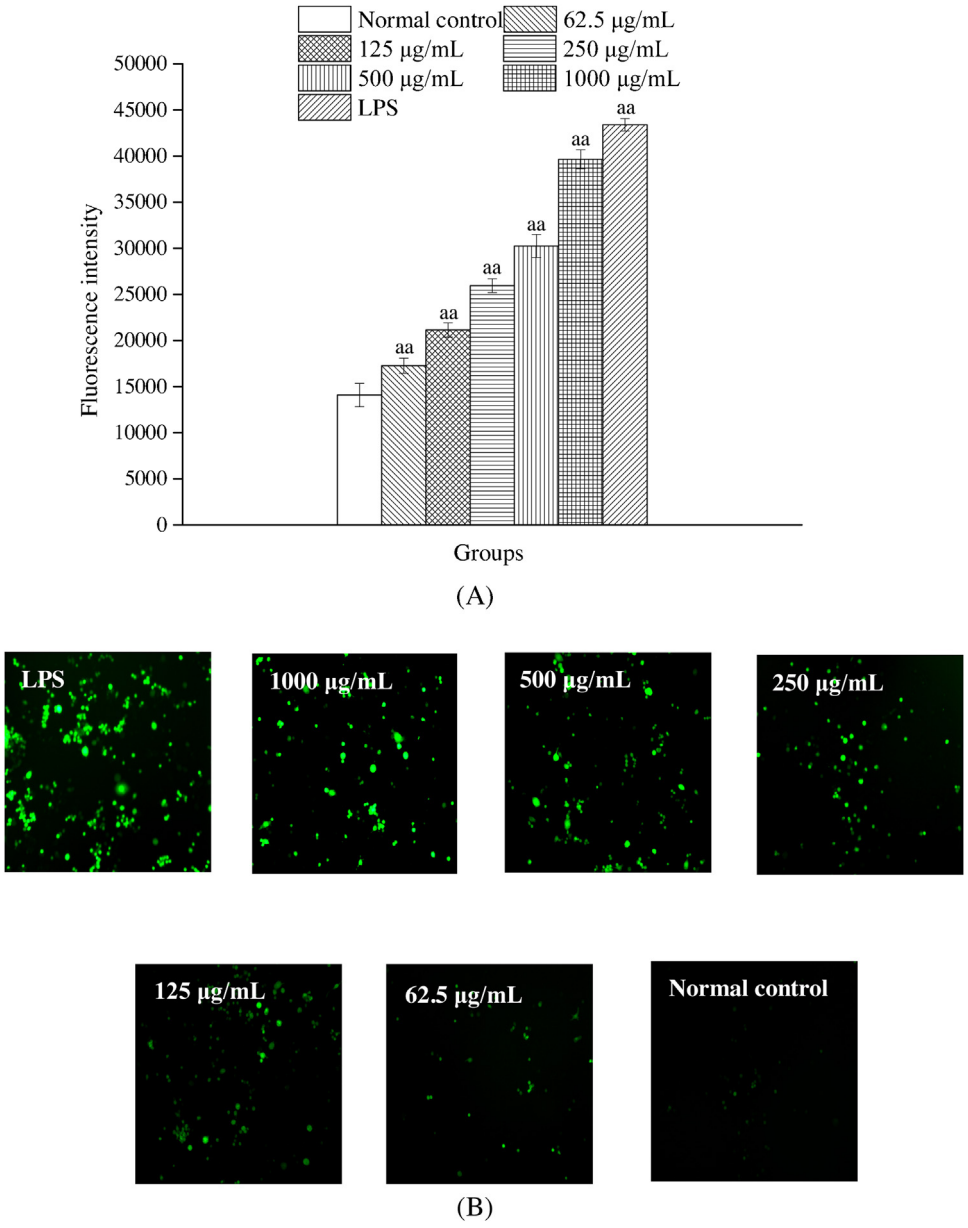

Fig. 4. (A) Effect of MP21 on intracellular ROS generation of RAW264.7; (B) Fluorescence microscopic images of cells stained for ROS. Each value is presented as mean ± S.D. ($n = 5$). $^{a}P < 0.05$ compared to normal control group. $^{aa}P < 0.01$ compared to normal control group.

activity. In general, polysaccharides are highly diversified in their glycosidic linkage, molecular mass, monosaccharide composition, conformation, degree of branching and other physicochemical properties, which together have effect on the immunomodulatory activity and other bioactivity [47]. Previous studies suggested that the branched spherical shape structures of polysaccharides were beneficial for their bioactivities [48]. Furthermore, in the study of other polysaccharides, the authors suggested that higher molecular weight polysaccharides could induce greater amount of NO production from RAW264.7 [46]. It also has been found that the bioactivity polysaccharides were mainly composed of rhamnose, galactose and arabinose. Lo et al. reported that mannose, arabinose, xylose, and galactose played a key role in the activation of macrophage, but not glucose [49]. In this study, MP21 were found to consist of similar monosaccharide compositions. Taken together, we can conclude that MP21 has significant immunomodulatory activity.

3.12. The protein expression of NF-κB p65

NF-κB is one of the most important regulators of gene expression in macrophages and usually stays in the cytoplasm due to its inactive non-covalent binding form with p50-p65-IκB trimer. When signals for the activation of NF-κB are received, serine residues in IκB are phosphorylated and dissociated from NF-κB, which is then transferred to the nucleus as an activated transcription factor [50]. After the dissociation of IκB, the binding sites of the p50–p65 dimer are exposed to combine with the κB motif. The NF-κB p65 subunit then transfers from the cytoplasm to the nucleus with potent activity leading to the transcription of a variety of genes, such as iNOS, ROS and macrophage-related cytokines [3]. In this study, the protein expression of nuclear NF-κB p65 was analyzed as a pathway potentially involved in the stimulation of macrophages by MP21. The NF-κB p65 protein showed higher expression after stimulation MP21 at 125 μg/mL to 1000 μg/mL (Fig. 5A), and the protein expression level at 1000 μg/mL was sig-

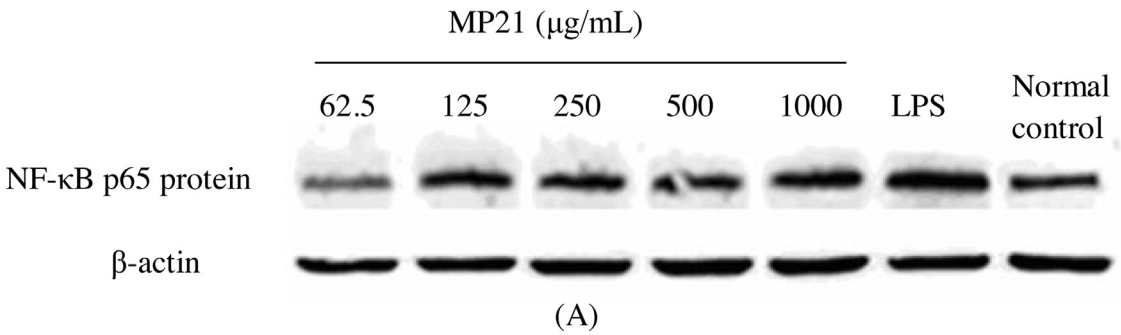

(A)

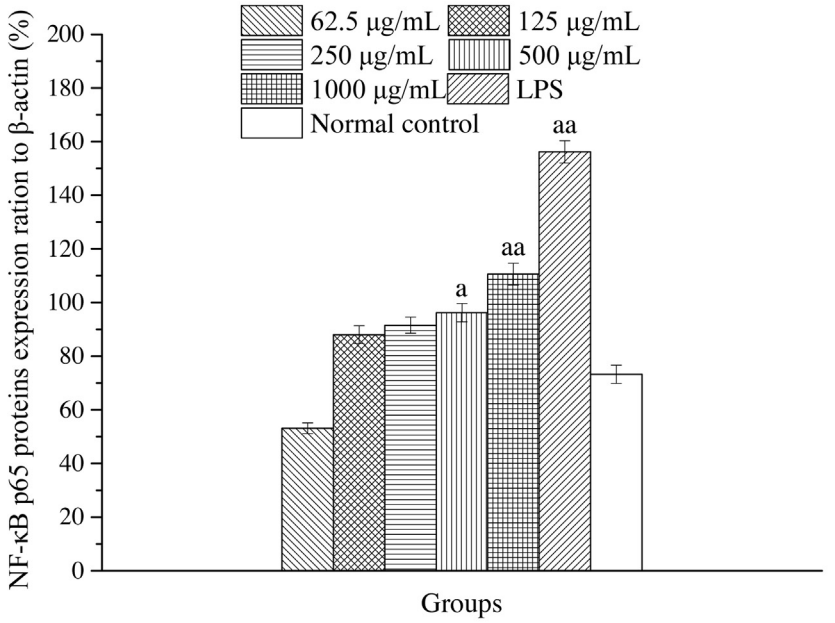

(B)

Fig. 5. (A) Effect of MP21 on the NF-κB p65 protein expression level in RAW 264.7; (B) Densitometry analyses are presented as NF-κB p65 proteins expression ratio to β-actin using Quantity One software. $^{a}P < 0.05$ compared to normal control group. $^{aa}P < 0.01$ compared to normal control group.

nificantly enhanced compared with that of the normal control group ($p < 0.01$) (Fig. 5B). In addition, the increasing trend in NF-κB p65 protein expression was consistent with analytical results of other functional indexes (*e.g.*, phagocytosis and NO, ROS, TNF-α and IL-1β secretion) of activated macrophages. Similar NF-κB activation activities were also observed in macrophages treated with polysaccharides from *Lentinula edodes*, *Ganoderma lucidum* and *C. militaris* [51]. Therefore, NF-κB signaling pathway might play a central role in macrophage-mediated immunomodulatory activity treated with polysaccharides and the effect of MP21 to activate the protein expression of NF-κB p65 provides further evidence that its immunomodulatory properties. Detailed intracellular signaling pathways will be further explored in the future.

4. Conclusions

In this study, a purified polysaccharide, MP21, was obtained from maca. MP21 had indirect cytotoxicity towards HepG-2 by stimulating macrophage responses. MP21 could activate macrophages by promoting phagocytosis and stimulating the production of NO, ROS and cytokines (TNF-α and IL-1β) in RAW264.7. The enhancement of NO secretion might be due to an increase in iNOS mRNA and protein levels. In addition, MP21 most likely enhanced macrophage activities by activating the NF-κB signaling pathway. All the data in this study provide evidence that MP21 has potent immunomodulatory properties and might be considered as a novel potential immunomodulator for use in drugs or functional foods to substitute for current pharmaceutical and food industry substances. The structure-function relationships and immune-regulatory mechanisms of MP21 will be studied in future investigations.

Acknowledgments

The authors are grateful for the financial support by Science and Technology Plan of Zhenjiang (GY2012002) and Graduate Innovative Projects in Jiangsu Province (KYLX_1073). We also appreciate Dr. Mohanmmed Takase and Samuel Jerry Cobbina for language polishing.

Appendix A. Supplementary data

Supplementary data associated with this article can be found, in the online version, at http://dx.doi.org/10.1016/j.procbio.2016.01.003.

References

[1] Y. Bai, P. Zhang, G. Chen, J. Cao, T. Huang, K. Chen, Macrophage immunomodulatory activity of extracellular polysaccharide (PEP) of Antarctic bacterium *Pseudoaltermonas* sp.S-5, Int. Immunopharmacol. 12 (2012) 611–617.

[2] J.H. Xiao, D.M. Xiao, D.X. Chen, Y. Xiao, Z.Q. Liang, J.J. Zhong, Polysaccharides from the medicinal mushroom *Cordyceps taii* show antioxidant and immunoenhancing activities in a D-galactose-induced aging mouse model, Evid-Based Complement. Altern. (2012) 273435.

[3] S.C. Sheu, Y. Lyu, M.S. Lee, J.H. Cheng, Immunomodulatory effects of polysaccharides isolated from *Hericium erinaceus* on dendritic cells, Process Biochem. 48 (2013) 1402–1408.

[4] S.J. Lee, H.K. Rim, J.Y. Jung, H.J. An, J.S. Shin, C.W. Cho, et al., Immunostimulatory activity of polysaccharides from Cheonggukjang, Food Chem. Toxicol. 59 (2013) 476–484.

[5] T.D. Wu, J. Xie, L.Y. Wang, Y.J. Ju, G.P. Lv, F. Leong, et al., Characterization of bioactive polysaccharides from *Cordyceps militaris* produced in China using saccharide mapping, J. Funct. Foods 9 (2014) 315–323.

[6] Y. Wang, Y.C. Wang, B. McNeil, Harvey L.M. Maca, An Andean crop with multi-pharmacological functions, Food Res. Int. 40 (2007) 783–792.

[7] G. Gonzales, A. Cordova, K. Vega, A. Chung, A. Villena, C. Gonez, et al., Effect of *Lepidium meyenii* (MACA) on sexual desire and its absent relationship with serum testosterone levels in adult healthy men, Andrologia 34 (2002) 367–372.

[8] M. Sandoval, N.N. Okuhama, F.M. Angeles, V.V. Melchor, L.A. Condezo, J. Lao, et al., Antioxidant activity of the cruciferous vegetable Maca (*Lepidium meyenii*), Food Chem. 79 (2002) 207–213.

[9] G.F. Gonzales, V. Vasquez, D. Rodriguez, C. Maldonado, J. Mormontoy, J. Portella, et al., Effect of two different extracts of red maca in male rats with testosterone-induced prostatic hyperplasia, Asian J. Androl. 9 (2007) 245–251.

[10] M.S. Lee, B.C. Shin, E.J. Yang, H.J. Lim, Ernst E. Maca, (*Lepidium meyenii*) for treatment of menopausal symptoms: a systematic review, Maturitas 70 (2011) 227–233.

[11] E.H. Choi, J.I. Kang, J.Y. Cho, S.H. Lee, T.S. Kim, I.H. Yeo, et al., Supplementation of standardized lipid-soluble extract from maca (*Lepidium meyenii*) increases swimming endurance capacity in rats, J. Funct. Foods 4 (2012) 568–573.

[12] K.J. Lee, K. Dabrowski, J. Rinchard, C. Gomez, L. Guz, C. Vilchez, Supplementation of maca (*Lepidium meyenii*) tuber meal in diets improves growth rate and survival of rainbow trout *Oncorhynchus mykiss* (Walbaum) alevins and juveniles, Aquacult. Res. 35 (2004) 215–223.

[13] S. Piacente, V. Carbone, A. Plaza, A. Zampelli, C. Pizza, Investigation of the tuber constituents of maca (*Lepidium meyenii* Walp.), J. Agric. Food Chem. 50 (2002) 5621–5625.

[14] M.M. McCollom, J.R. Villinski, K.L. McPhail, L.E. Craker, S. Gafner, Analysis of macamides in samples of Maca (*Lepidium meyenii*) by HPLC–UV–MS/MS, Phytochem. Anal. 16 (2005) 463–469.

[15] A. Dini, G. Migliuolo, L. Rastrelli, P. Saturnino, O. Schettino, Chemical composition of *Lepidium meyenii*, Food Chem. 49 (1994) 347–349.

[16] S.H. Zha, Q.S. Zhao, J.J. Chen, L.W. Wang, G.F. Zhang, H. Zhang, B. Zhao, Extraction, purification and antioxidant activities of the polysaccharides from maca (*Lepidium meyenii*), Carbohydr. Polym. 111 (2014) 584–587.

[17] M. Dubois, K.A. Gilles, J.K. Hamilton, P.T. Rebers, F. Smith, Colorimetric method for determination of sugars and related substances, Anal. Chem. 28 (1956) 350–356.

[18] N. Blumencrantz, G. Asboe-Hansen, New methods for quantitative determination of uronic acids, Anal. Biochem. 54 (1973) 484–489.

[19] M.M. Bradford, A rapid and sensitive method for the quantitation of microgram quantities of protein utilizing the principle of protein-dye binding, Anal. Biochem. 72 (1976) 248–254.

[20] L.Q. Yang, T. Zhao, H. Wei, M. Zhang, Y. Zou, G.H. Mao, et al., Carboxymethylation of polysaccharides from *Auricularia auricula* and their antioxidant activities *in vitro*, Int. J. Biol. Macromol. 49 (2011) 1124–1130.

[21] K. Wang, W. Li, X. Rui, X. Chen, M. Jiang, M. Dong, Characterization of a novel exopolysaccharide with antitumor activity from *Lactobacillus plantarum* 70810, Int. J. Biol. Macromol. 63 (2014) 133–139.

[22] L. Liu, Y.M. Lu, X.H. Li, L.Y. Zhou, D. Yang, L.M. Wang, et al., A novel process for isolation and purification of the bioactive polysaccharide TLH-3′ from *Tricholoma lobayense*, Process Biochem. 50 (2015) 1146–1151.

[23] C.H. Liu, C.H. Wang, Z.L. Xu, Y. Wang, Isolation, chemical characterization and antioxidant activities of two polysaccharides from the gel and the skin of *Aloe barbadensis* Miller irrigated with sea water, Process Biochem. 42 (2007) 961–970.

[24] J.N. Zhang, Q.P. Xiong, S.J. Li, X. Li, J.P. Chen, M. Cao, et al., A comparison study on polysaccharides from novel hybrids of *Amomum villosum* and its female parent, Int. J. Biol. Macromol. 81 (2015) 396–399.

[25] M. Cerná, A.S. Barros, A. Nunes, S.M. Rocha, I. Delgadillo, J. opíková, et al., Use of FT-IR spectroscopy as a tool for the analysis of polysaccharide food additives, Carbohydr. Polym. 51 (2003) 383–389.

[26] A.K. Siddhanta, R. Meena, G. Prasad, M.U. Chhatbar, G.K. Mehta, M.D. Oza, S. Kumar, K. Prasad, Development of carbohydrate polymer based new hydrogel materials derived from seaweed polysaccharides, in: I. Ryouichi, M. Youta (Eds.), Carbohydrate Polymers: Development, Properties and Applications, 2010, pp. 555–582.

[27] S. Chen, H. Chen, Z. Wang, J. Tian, J. Wang, Structural characterization and antioxidant properties of polysaccharides from two *Schisandra* fruits, Eur. Food Res. Technol. 237 (2013) 691–701.

[28] Y.S. Zhang, Conformational study of polysaccharide, J. Northeast Normal Univ. 2 (1998) 55–60.

[29] S. Bystricky, S.C. Szu, M. Gotoh, P. Kovac, Circular dichroism of the O-specific polysaccharide of *Vibrio cholerae* O1 and some related derivatives, Carbohydr. Res. 270 (1995) 115–122.

[30] Y. Zhu, Q. Li, G.H. Mao, Y. Zou, W.W. Feng, D.H. Zheng, et al., Optimization of enzyme-assisted extraction and characterization of polysaccharides from *Hericium erinaceus*, Carbohydr. Polym. 101 (2014) 606–613.

[31] H.L. Zeng, S. Miao, Y. Zhang, S. Lin, Y.Y. Jian, Y.T. Tian, et al., Isolation, preliminary structural characterization and hypolipidemic effect of polysaccharide fractions from *Fortunella margarita* (lour) swingle, Food Hydrocolloid 52 (2016) 126–136.

[32] Z.P. Huang, Y.A. Huang, X.B. Li, L.N. Zhang, Molecular mass and chain conformations of *Rhizoma Panacis Japonici* polysaccharides, Carbohydr. Polym. 78 (2009) 596–601.

[33] M.L. Cho, C. Yang, S.M. Kim, S.G. You, Molecular characterization and biological activities of water-soluble sulfated polysaccharides from *Enteromorpha prolifera*, Food Sci. Biotechnol. 19 (2010) 525–533.

[34] G. Wang, J. Zhao, J.W. Liu, Y.P. Huang, J.J. Zhong, W. Tang, Enhancement of IL-2 and IFN-γexpression and NK cells activity involved in the anti-tumor effect of ganoderic acid Me in vivo, Int. Immunopharmacol. 7 (2007) 864–870.

[35] G.H. Mao, Y. Ren, W.W. Feng, Q. Li, H.Y. Wu, J. Dun, Antitumor and immunomodulatory activity of a water-soluble polysaccharide from *Grifola frondosa*, Carbohydr. Polym. 134 (2015) 406–412.

[36] J.R. Chen, Z.Q. Yang, T.J. Hu, Z.T. Yan, T.X. Niu, L. Wang, et al., Immunomodulatory activity *in vitro* and *in vivo* of polysaccharide from *Potentilla anserina*, Fitoterapia 81 (2010) 1117–1124.

[37] T. Zhao, G.H. Mao, R.W. Mao, Y. Zou, D.H. Zheng, W.W. Feng, et al., Antitumor and immunomodulatory activity of a water-soluble low molecular weight polysaccharide from *Schisandra chinensis* (Turcz) Baill, Food Chem.Toxicol. 55 (2013) 609–616.

[38] Q. Yu, S.P. Nie, W.J. Li, W.Y. Zheng, P.F. Yin, D.M. Gong, et al., Macrophage immunomodulatory activity of a purified polysaccharide isolated from *Ganoderma atrum*, Phytother. Res. 27 (2013) 186–191.

[39] T. Kadowaki, S. Ohno, Y. Taniguchi, H. Inagawa, C. Kohchi, G.I. Soma, Induction of nitric oxide production in RAW264.7 cells under serum-free conditions by O-antigen polysaccharide of lipopolysaccharide, Anticancer Res. 33 (2013) 2875–2879.

[40] S. Lee, D.S. Kwon, K.R. Lee, J.M. Park, S.J. Ha, E.K. Hong, Mechanism of macrophage activation induced by polysaccharide from *Cordyceps militaris* culture broth, Carbohydr. Polym. 120 (2015) 29–37.

[41] M. Jin, S.J. Suh, J.H. Yang, Y. Lu, S.J. Kim, S. Kwon, et al., Anti-inflammatory activity of bark of *Dioscorea batatas* DECNE through the inhibition of iNOS and COX-2 expressions in RAW264.7 cells via NF-κB and ERK1/2 inactivation, Food Chem. Toxicol. 48 (2010) 3073–3079.

[42] J.S. Lee, E.K. Hong, Immunostimulating activity of the polysaccharides isolated from *Cordyceps militaris*, Int. Immunopharmacol. 11 (2011) 1226–1233.

[43] Q. Fang, J.F. Wang, X.Q. Zha, S.H. Cui, L. Cao, J.P. Luo, Immunomodulatory activity on macrophage of a purified polysaccharide extracted from *Laminaria japonica*, Carbohydr. Polym. 134 (2015) 66–73.

[44] T. Noguchi, ROS-dependent activation of ASKI in inflammatory signaling, J. Oral Biosci. 50 (2008) 107–114.

[45] L.A.J. O'Neill, D.G. Hardie, Metabolism of inflammation limited by AMPK an pseudo-starvation, Nature 493 (2013) 346–355.

[46] I.A. Schepetkin, G. Xie, L.N. Kirpotina, R.A. Klein, M.A. Jutia, M.T. Quinn, Macrophage immunomodulatory activity of polysaccharides isolated from *Opuntia polyacantha*, Int. Immunopharmacol. 8 (2008) 1455–1466.

[47] A.E.E. Hesham, H.K. Rajni, Mushroom immunomodulators: unique molecules with unlimited applications, Trends Biotechnol. 31 (2013) 668–677.

[48] Q. Han, Q.Y. Yu, J. Shi, C.Y. Xiong, Z.J. Ling, P.M. He, Molecular characterization and hypoglycemic activity of a novel water-soluble polysaccharide from tea (*Camellia sinensis*) flower, Carbohydr. Polym. 86 (2011) 797–805.

[49] T.C.T. Lo, Y.H. Jiang, A.L.J. Chao, C.A. Chang, Use of statistical methods to find the polysaccharide structural characteristics and the relationships between monosaccharide composition ratio and macrophage stimulatory activity of regionally different strains of *Lentinula edodes*, Anal. Chim. Acta 584 (2007) 50–56.

[50] S. Beinke, S.C. Ley, Functions of NF-κB1 and NF-κB2 in immune cell biology, Biochem. J. 382 (2004) 393–409.

[51] J.M. Park, T. Kunieda, T. Kubo, The activity of Mblk-1, a mushroom body-selective transcription factor from the honeybee, is modulated by the ras/MAPK pathway, J. Biol. Chem. 278 (2003) 18689–18694.